ORIGINAL ARTICLE

Persistent Neuroinflammatory Effects of Serial Exposure to Stress and Methamphetamine on the Blood-Brain Barrier

Nicole A. Northrop · Bryan K. Yamamoto

Abstract Studies of methamphetamine (Meth)-induced neurotoxicity have traditionally focused on monoaminergic terminal damage while more recent studies have found that stress exacerbates these damaging effects of Meth. Similarities that exist between the mechanisms that cause monoaminergic terminal damage in response to stress and Meth and those capable of producing a disruption of the blood-brain barrier (BBB) suggest that the well-known high co-morbidity of stress and Meth could produce long-lasting structural and functional BBB disruption. The current studies examined the role of neuroinflammation in mediating the effects of exposure to chronic stress and/or Meth on BBB structure and function. Rats were pre-exposed to chronic unpredictable stress (CUS) and/or challenged with Meth. Twenty-four hours after the treatment of Meth in rats pre-exposed to CUS, occludin and claudin-5 immunoreactivity were decreased while truncation of β-dystroglycan, as well as FITC-dextran and water extravasation was increased. All changes other than β-dystroglycan and edema persisted 7 days later, occurred with increases in GFAP and COX-2, and were blocked by ketoprofen after Meth treatment. In addition, persistent increases in FITC-dextran extravasation were prevented by treatment with an EP1 receptor antagonist after Meth exposure. The results indicate that CUS and Meth synergize to produce long-lasting structural and functional BBB disruptions that are mediated by cyclooxygenase and protracted increases in inflammation. These results suggest that stress and Meth can synergize to produce a long-lasting vulnerability of the brain to subsequent environmental insults resulting from the persistent breach of the BBB.

N. A. Northrop · B. K. Yamamoto (✉)
Department of Neurosciences, University of Toledo College of Medicine, Health Sciences Campus,
30000 Arlington Avenue, Mailstop 1007,
Toledo, OH 43614, USA
e-mail: bryan.yamamoto@utoledo.edu

Introduction

The psychostimulant, methamphetamine (Meth), is a widely abused drug that produces long-term neuronal damage in humans, non-human primates and rodents. PET and proton magnetic resonance spectroscopy studies of abstinent human Meth abusers illustrate decreases in the dopamine transporter (DAT) (McCann et al. 1998; Volkow et al. 2001a) and the neuronal marker, N-acetylaspartate (Ernst et al. 2000), biomarkers indicative of neurotoxicity. In addition, long-term decreases in serotonin transporter (SERT), vesicular monoamine transporter-2, tyrosine and tryptophan hydroxylase immunoreactivity, and dopamine (DA) and serotonin (5-HT) tissue content (Hotchkiss and Gibb 1980; Ricaurte et al. 1980; Wagner et al. 1980; Eyerman and Yamamoto 2007) are observed in rodents. While most studies have focused on Meth-induced monoaminergic terminal damage caused by oxidative stress and neuroinflammation (Yamamoto et al. 2010), there are less studied neurotoxicities that could be mediated by similar mechanisms.

The same mechanisms of Meth-induced damage to monoaminergic terminals may also be responsible for an increase in the permeability of the blood-brain barrier (BBB) (Abbott 2000; Ramirez et al. 2009). Moreover, acute BBB disruption is caused by seizures and hyperthermia associated with high dose Meth exposure (Bowyer and Ali 2006; Kiyatkin et al. 2007; Kiyatkin and Sharma 2009a, b). The increased permeability may result from alterations to structural proteins. Normally, brain endothelial cells restrict paracellular transport of molecules from blood to brain parenchyma by the presence of tight junctions, comprised of the transmembrane structural proteins, claudin-3,-5,

occludin and junctional adhesion molecule. In addition, tight junctions are stabilized by intracellular proteins, such as zona occludens (ZO), and transmembrane proteins, such as β-dystroglycan, which crosslink astrocytic endfeet and endothelial cells to the basal lamina. In fact, Meth decreases occludin, claudin-5 and ZO-1 protein in cultured brain microvascular endothelial cells (Ramirez et al. 2009; Abdul Muneer et al. 2011) and mouse brain (Martins et al. 2011), suggesting that Meth can increase permeability via changes in BBB structural proteins. However, the mechanisms underlying these possible changes under in vivo conditions are unknown.

Neuroinflammation mediates Meth toxicity to monoamine terminals (Thomas et al. 2004) but its role in Meth-induced BBB disruption is unknown. The inflammatory mediator, cyclooxygenase (COX) has been implicated in BBB disruption and is increased in response to Meth (Kita et al. 2000; Thomas and Kuhn 2005). Furthermore, nonselective inhibition of COX attenuated TNFα-induced BBB disruption (Candelario-Jalil et al. 2007) whereas antagonism of prostaglandin E2 receptor, EP1, reduced the disruption of the structure and function of the BBB in a stroke model (Fukumoto et al. 2010). Collectively, these data suggest that COX and its downstream consequences can mediate Meth-induced BBB disruption.

COX is increased in the brain by physical and psychological stressors (Yamagata et al. 1993; Madrigal et al. 2003) and environmental stress potentiates METH toxicity (Tata and Yamamoto 2007). The interaction between stress and drugs of abuse is particularly relevant as stress and drug abuse are highly comorbid. Therefore, stress may enhance Meth-induced BBB disruption through COX and neuroinflammation. It is hypothesized that serial exposure to chronic unpredictable stress and moderate doses of Meth will produce acute and persistent structural and functional disruptions of the BBB through changes in COX activity.

Materials and methods

Animals

Male Sprague Dawley rats (180–275 g, Harlan Indianapolis, IN) were used in all experiments. Rats were housed 2 to 3 per cage, in clear plastic containers (45×24×20 cm), and allowed 4–5 days to acclimate to the animal colony before any experimentation. The environment in which the rats were housed was under a 12 hr light/dark cycle, temperature (23±1 °C) and humidity (40±5 %) controlled and rats had ad libitum access to food and water. All procedures were carried out in accordance with the National Institutes of Health Guide for the Care and Use of Laboratory Animals and approved by the University of Toledo Institutional

Animal Care and Use Committee. Efforts were made to minimize the number of rats used as well as to minimize the amount of suffering each rat might endure.

Chronic Unpredictable Stress (CUS) paradigm and drug treatments

Rats were either handled daily or exposed to the chronic unpredictable stress (CUS) paradigm, which consisted of exposure to a variety of mild stressors at varying times during the day, for 10 days. The stress schedule was as follows: day 1, 50 minute cold room (10:00 h) and 30 minute cage agitation (14:00 h); day 2, 3 hrs lights off (9:00 h) and lights on overnight; day 3, 1 hr restraint (11:00 h) and food and water deprivation (17:00 h–8:00 h); day 4, 1 hr cage agitation (10:00 h) and 50 minute cold room (15:00 h); day 5, 15 minute cold room isolation (14:00 h) and isolation overnight (14:15 h–8:00 h); day 6, 1 hr restraint (9:00 h) and lights on overnight; day 7, 3 hrs lights off (10:00 h) and food and water deprivation (17:00 h–8:00 h); day 8, 1 hr cage agitation (11:00 h) and isolation overnight (16:00 h–8:00 h); day 9, 15 minute cold room isolation (9:00 h) and lights on overnight; day 10, 3 hrs lights off (10:00 h) and 20 minute cage agitation (15:00 h). This CUS paradigm has been used previously (Stein-Behrens et al. 1994; Haile et al. 2001; Matuszewich and Yamamoto 2004) and does not result in adaptation, but produces increased levels of plasma corticosterone (Johnson and Yamamoto 2009).

On the day after the last stressor, rats received drug treatment. (+) Methamphetamine-hydrochloride (Meth) was purchased from Sigma (St. Louis, MO, Cat. M-8750) and dissolved in 0.9 % NaCl (saline). Meth was administered to rats at a dose of 7.5 mg/kg, intraperitoneally (ip) every 2 hrs for a total of 4 injections. Controls for Meth treatment were rats treated with 4 ip injections of saline (1 mL/kg), one injection given every 2 hrs. The total dose administered to the rat in the current study is 30 mg/kg. Accounting for the approximately 6-fold higher metabolic rate of the rat, the approximate human dose, would be 5 mg/kg or 350 mg/70 kg human. This dose is applicable to human drug use since humans administer anywhere from 50 mg to 1,000 mg of Meth per day (McKetin et al. 2006; Cruickshank and Dyer 2009). In addition, the dose of Meth was chosen because, in combination with 10 days of CUS, it causes damage to the dopaminergic system (Tata et al. 2007), to a similar extent to that observed in the human brain, as measured by DAT binding (Volkow et al. 2001a; Volkow et al. 2001b).

The nonselective COX inhibitor, ketoprofen (5 mg/kg) was purchased from Sigma (St. Louis, MO, Cat. K1751). Ketoprofen was dissolved in 100 % transcutol (generous gift from Gattefossé Corporation, Paramus, NJ, USA) and

diluted 1:4 with Millipore water, resulting in a final solution of 2.5 mg/mL ketoprofen in 25 % transcutol. The vehicle control for ketoprofen was 2 mL/kg of 25 % transcutol. During saline or Meth administration, ketoprofen was injected subcutaneously (sc) at a dose of 5 mg/kg ketoprofen, 1 hr before each Meth or saline injection (Ketoprofen During). The dose and treatment paradigm of 5 mg/kg of ketoprofen was chosen based on a previous study that observed an attenuation of Meth-induced decreases in DAT immunoreactivity (Asanuma et al. 2003). Ketoprofen administration after saline or Meth treatment consisted of sc injections of 5 mg/kg ketoprofen twice a day, starting 24 hr after Meth or saline treatment and continued for 6 days (Ketoprofen Post). The administration of ketoprofen twice a day was chosen based on the 12 hr half-life of ketoprofen (Foster and Jamali 1988). Ketoprofen during and after Meth or saline treatment consisted of 5 mg/kg ketoprofen injections 1 hr before each Meth or Saline injections and twice a day, starting 24 hr after the start of Meth treatment and continuing for the 6 days after Meth or saline treatment (Ketoprofen During &Post).

A separate group of rats received the EP1R antagonist, SC-51089 (Cayman Chemical, Ann Arbor, MI, Cat. 10011561), after treatment to investigate the role of the EP1R in Stress + Meth-induced long-term BBB disruptions. Rats received SC-51089 at a dose of 10 μg/kg ip, twice a day, starting 24 hr after the initiation of Meth treatment and continuing for the 6 days after Meth or saline treatment. SC-51089 was dissolved in 0.02 % DMSO. DMSO (0.02 %) was used as the vehicle control for these experiments. The dose of SC-51089 was chosen based on its ability to inhibit NMDA and ischemia-induced lesions (Kawano et al. 2006) and prevent ischemia-induced BBB disruption (Fukumoto et al. 2010).

During drug treatments, rectal temperatures were measured using a digital thermometer with rectal probe (Thermalert TH-8; Physitemp Instruments Inc., Clifton, NJ) prior to the first injection and 1 hr after each injection. Rats that reached temperatures greater than 41 °C were cooled briefly by placing ice packs on top of their cage covers while their temperatures were closely monitored. Cooling was complete when rats reached temperatures less than 40.5 °C in order to maintain hyperthermia while minimizing lethality.

Rats used for measurements of occludin, claudin-5, β-dystroglycan, brain water content, glial fibrillary acidic protein (GFAP) and COX-2 were killed via live decapitation at either 24 hrs or 7 days after drug treatments. Brains were immediately removed from the skull and dissected on top of a cold, dry non-porous surface. Fresh, non-frozen tissue was used for capillary isolation and measurement of brain water content (see below) while remaining tissue was frozen on dry ice and stored at −80 °C prior to measurement of β-dystroglycan, GFAP and COX-2 via Western Blot (see below). Separate groups of animals were used for functional measurement of BBB permeability, as measured by FITC-dextran extravasation, at 24 hrs and 7 days (see below).

Isolation of brain capillaries

Brain capillaries were isolated using a modified protocol from Yousif et al. (2007). Immediately after decapitation, brains were removed from the skull and cerebellum and circumventricular organs were dissected free. The remaining cortical tissue was placed into cold Hanks' Balanced Salt Solution 1× (HBSS) and samples were kept on ice or at 4 °C throughout the isolation procedure. Meninges and large blood vessels were removed in cold HBSS and the remaining tissue was minced in 500 μL HBSS. Homogenate was centrifuged at 1,000 g for 10 min, supernatant decanted and pellet resuspended in 17.5 % dextran (64–76 kDa, Sigma) by pipetting up and down. This dextran homogenate was centrifuged at 4,400 g at 4 °C for 15 min to produce a pellet of capillaries. The supernatant was collected along with floating tissue pieces, placed into a separate tube, and centrifuged at 4,400 g for 15 min at 4 °C that resulted in a second pellet containing capillaries. After the supernatants were decanted, both remaining pellets were resuspended in ice-cold HBSS and combined. This mixture was then filtered through 100 μm nylon mesh (Spectrum Laboratories, Inc., Rancho Dominguez, CA) to remove large blood vessels. The filtrate containing the capillaries was centrifuged at 1,000 g for 5 min to concentrate the capillaries.

Western blotting for occludin, claudin-5, β-dystroglycan, GFAP and COX-2

Occludin and claudin-5, as well as COX-2 in some cases, were measured in isolated capillary protein. Isolated capillaries described above were resuspended in a urea buffer, containing 6 M urea, 10 mM Tris, 1 mM DTT, 5 mM $MgCl_2$, 5 mM EDTA-NA_4, 150 mM NaCl and protease inhibitor cocktail, with a pH of 8.0, and were incubated at 4 °C for two nights to extract capillary proteins (Hawkins et al. 2004). Capillary protein samples were diluted 1:4 with Novex 4× LDS sample buffer (Invitrogen, Carlsbad, CA) and boiled at 85 °C for 10 minutes. Bradford protein assay (BioRad, Hercules, CA) was used to measure total capillary protein.

β-dystroglycan, GFAP and COX-2 protein expression was measured in whole tissue. Brain tissue was homogenized in RIPA buffer (0.1 M PBS, 1 % Igepal, 0.5 % sodium deoxycholate, and 0.1 % sodium dodecyl sulfate) with 1× Halt protease inhibitor cocktail (Thermo Scientific, Rockford, IL, Cat. 78430) and centrifuged at 12,000 rpm for 5 minutes to pellet insoluble material. Bradford assay

(BioRad, Hercules, CA) was used to measure total protein in samples, samples were diluted 1:4 with Novex 4× LDS sample buffer (Invitrogen, Carlsbad, CA) and heated to 80 °C for 5 minutes.

Equal amounts of protein for each sample (30 μg of capillary protein for occludin, claudin-5 and COX-2, 60 μg of whole cortical protein for β-dystroglycan, 30 ug of whole cortical protein for COX-2, and 15 μg of whole cortical protein for GFAP) were loaded onto a NuPAGE Novex 4–12 % Bis-Tris gel (Invitrogen, Carlsbad, CA) for electrophoresis. Proteins were transferred onto polyvinylidene fluoride (PVDF) membranes. Membranes were blocked for 3 hrs at room temperature, with Tris-buffered saline (TBS) (10 mM Tris, 150 mM NaCl), containing 0.5 % Tween-20 and 5 % non-fat powdered milk. Membranes were then incubated with primary antibodies (mouse anti-occludin, 1:500, (Invitrogen, Carlsbad, CA, Cat. 331500); mouse anti-claudin-5, 1:500, (Invitrogen, Carlsbad, CA, Cat. 352500); mouse anti-β-dystroglycan, 1:500, (Leica Microsystems, Novocastra Reagents, Buffalo Grove, IL, Cat. B-DG-CE); mouse anti-GFAP, 1:2000, (Boehringer Mannheim, Cat. 814369); goat anti-COX-2, 1:500, (Santa Cruz, Cat. sc-1746) mouse anti-α-tubulin, 1:3000, (Sigma, St. Louis, MO, Cat. T6074)) in blocking buffer for approximately 18 hrs at 4 °C. Following 3, 5 min, washes with TBS containing Tween-20 (TBS-T) (0.5 % Tween for occuldin, claudin-5, GFAP, COX-2 and α-tubulin; 0.1 % Tween for β-dystroglycan), membranes were incubated with horseradish peroxidase (HRP)-conjugated secondary antibodies (goat anti-mouse IgG, 1:2500, (Santa Cruz) or rabbit anti-goat IgG, 1:2500, (Santa Cruz)) in blocking buffer for 1 hr at room temperature. Membranes were then washed 3 times, each for 5 min, with TBS-T.

Membranes were incubated in HyGLO enhanced chemiluminescence (ECL) (Denville Scientific Inc., Metuchen, NJ), for antibody detection. A Fuji LAS-4000 mini system (FujiFilm Corp. Life Science Division, Tokyo, Japan) was used to image chemiluminescence and optical density was quantified using Multi Gauge software (FujiFilm Corp. Life Science Division, Tokyo, Japan).

Occludin, claudin-5, GFAP and COX-2 were normalized to the internal loading control, α-tubulin. Results were calculated and expressed as a percent of control group. β-dystroglycan is presented as truncated β-dystroglycan and expressed as a percent of No Stress + Saline controls. Truncation of β-dystroglycan was calculated by taking a ratio of truncated to full form β-dystroglycan.

Measurement of brain water content

Freshly dissected cortical tissue was immediately weighed (wet weight) after live decapitation and placed in a desiccator at 70 °C for 72 hrs. This time was chosen because loss of water weight was maximal by this time. After the 72 hrs, tissue was weighed again (dry weight). The percent of water was calculated as follows: % water = (wet weight-dry weight)/wet weight × 100.

FITC-dextran extravasation

Leakage of FITC-dextran from brain vasculature into parenchyma was used to determine the extent of BBB permeability. A protocol similar to Zhao et al. (2007) was used. Briefly, 24 hr or 7 days after drug treatment, a solution of ketamine (75 mg/kg) (Hospira, INC., Lake Forest, IL) and xylazine (5 mg/kg) (Lloyd Laboratories, Shenandoah, Iowa) was injected intramuscularly into rats. The rat heart was exposed and heparin (35 USP units) (APP Pharmaceuticals, LLC, Schauburg, IL) was injected into the left ventricle. Immediately following the heparin injection, 12 mL of FITC labeled 10,000 Da dextran (10 mg/mL in 0.1 M PBS) (Sigma, St. Louis, MO, Cat. FD10S) was infused into the left ventricle at a rate of 5 mL/minute and the right atrium was severed. Immediately following the intracardial perfusion, brains were removed from the skull and placed into 4 % paraformaldehyde (PFA). After 3 days in PFA, brains were cryoprotected by placing them into 10 % glycerol for 24 hr and then 20 % glycerol for 24 hr. Brains were then flash frozen in 2-methylbutane over dry ice.

Brains were sliced at a thickness of 50 μm using a cryostat (Microm HM 550; Thermo Scientific, Waltham, MA). Slices were mounted onto gelatin coated slides and cover-slipped with fluoromount. Slices were imaged using a Leica SP5 confocal microscope and the standard Leica Applications Suite Advanced Fluorescence (LAS AF) Software. Parameters used to image included an excitation wavelength of 488 nm, a collection wavelength of 504–556 nm and z-step size of 4.00 μm. Exposure, gain and offset remained constant for all images. Four 20× images of regions of the cortex were captured per rat, from 3 brain slices, in order to analyze FITC-dextran extravasation. At the time of analysis, the investigator was blind to the treatment.

In order to quantify FITC-dextran extravasation, extra-capillary fluorescence in each image was quantified using ImageJ software. First, brightly stained discrete areas, indicative of capillaries, were removed from each image by setting the outlier settings of threshold and radius the same for all images. Threshold and radius settings were chosen based on the settings that removed capillary staining from control slice images. The average intensity of the remaining fluorescence of the entire area imaged was then measured using ImageJ. The fluorescence values of the 4 images, taken from 3 slices from each rat, were averaged for each individual rat. The mean intensity of fluorescence was expressed as a percent of control and is indicative of FITC-dextran extravasation.

Statistical analysis

Statistical analysis was performed using Sigma Plot 11. Body temperatures were analyzed using a two-way analysis of variance (ANOVA) with repeated measures, followed by Tukey's post hoc analysis. A two-way ANOVA was used to determine significant effects of stress and Meth on occludin, claudin-5, β-dystroglycan, GFAP and COX-2 protein expression and brain water content and FITC-dextran extravasation, at 24 hr after treatment. A two-way ANOVA was also used to determine significant effects of stress and Meth on GFAP and COX-2 protein expression 7 days after treatment. When a significant two-way interaction was identified, Tukey's post hoc analysis were used to identify significant differences between treatment groups. A one-way ANOVA within treatment followed by post hoc analysis using the Bonferroni's Multiple Comparisons test were used to determine the effects of ketoprofen on Stress + Meth-induced changes in occludin, claudin-5 and COX-2 protein immunoreactivity, truncation of β-dystroglycan, brain water content and FITC-dextran extravasation at 7 days after Meth treatment. To determine the effects of the EP1 receptor antagonist, SC-51089, on Stress + Meth-induced increases in FITC-dextran extravasation at 7 days after treatment, a two-way ANOVA, with Tukey's post-hoc analysis, was used. For all experiments, statistical significance was set at $p<0.05$.

Results

Effects of stress on meth-induced hyperthermia

The effects of Meth treatment and prior exposure to stress on body temperatures are illustrated in Fig. 1. When body temperatures were measured 1 hr after each Meth or saline injection, Meth administration (7.5 mg/kg ip × 4 every 2 hr) produced an increase in core body temperatures of ~1 °C, compared to saline controls. In addition, prior exposure to 10 days of chronic unpredictable stress enhanced the effects of Meth on body temperature and increased body temperature by ~1 °C, compared to No Stress + Meth treated rats. These effects were revealed by a significant effect of treatment over time ($F_{12,149}=10.76$, $p<0.001$) in a two-way repeated measures ANOVA. Post-hoc analysis indicated that No Stress + Meth treated rats were significantly different from No Stress + Saline at 3 hr ($q=4.66$, $p<0.01$), 5 hr ($q=5.17$, $p<0.01$) and 7 hr ($q=5.46$, $p<0.001$) after the first Meth injection and were significantly different from Stress + Saline groups at 5 hr ($q=3.94$, $p<0.05$) and 7 hr ($q=3.86$, $p<0.05$) after the first Meth injection. In addition, post-hoc analyses indicated that Stress + Meth groups were significantly different from No Stress + Saline groups at 3 hr ($q=$
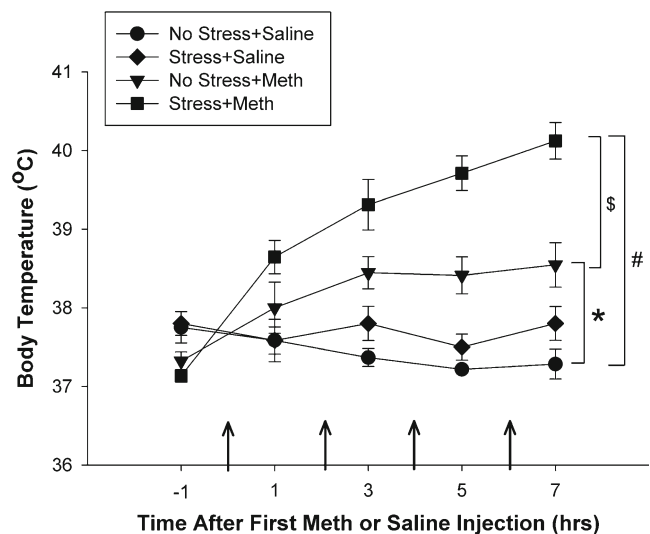

Fig. 1 Rectal temperatures after exposure to stress and Meth. Meth or saline was administered to previously stressed or control rats. Body temperatures were measured before and every hr after a Meth or saline injection, indicated by the arrows on the x-axis. Meth significantly increased body temperature over time (*, $p<0.01$) and prior exposure to 10 days of CUS significantly increased body temperature compared to No Stress + Saline (#, $p<0.001$) and No Stress + Meth ($, $p<0.05$). ($n=8$–10 in each group)

8.41, $p<0.001$), 5 hr ($q=10.79$, $p<0.001$) and 7 hr ($q=12.28$, $p<0.001$) after the first Meth injection and Stress + Saline groups at 3 hr ($q=6.54$, $p<0.001$), 5 hr ($q=9.57$, $p<0.001$) and 7 hr ($q=10.05$, $p<0.001$) after the first Meth injection. Furthermore, Stress + Meth treated rats were also significantly different from No Stress + Meth treated rats at 3 hr ($q=4.19$, $p<0.05$), 5 hr ($q=6.29$, $p<0.001$) and 7 hr ($q=7.63$, $p<0.001$) after the first Meth injection. Stress + Saline rats did not differ from No Stress + Saline rats.

Effects of stress and meth on acute alterations of BBB transmembrane structural proteins

Figure 2a illustrates the quantification of occludin protein expression in isolated capillaries, 24 hr after treatment with Meth or saline. Figure 2c is a representative Western Blot image of occludin (57 kDa) and the loading control, α-tubulin (50 kDa). The combination of stress and Meth significantly decreased protein expression of occludin in isolated capillaries by 40±6 %, compared to No Stress + Saline controls. These effects were revealed by a significant effect of stress ($F_{1,36}=13.82$, $p<0.001$), Meth ($F_{1,36}=5.76$, $p<0.05$), and a significant interaction of Meth treatment and stress ($F_{1,36}=4.89$, $p<0.05$). Post-hoc analysis revealed a significant difference between Stress + Meth and No Stress + Meth ($q=5.87$, $p<0.001$) as well as Stress + Meth and Stress + Saline ($q=4.57$, $p<0.01$), but no effects of stress in saline treated rats or the effects of Meth in no stress rats.
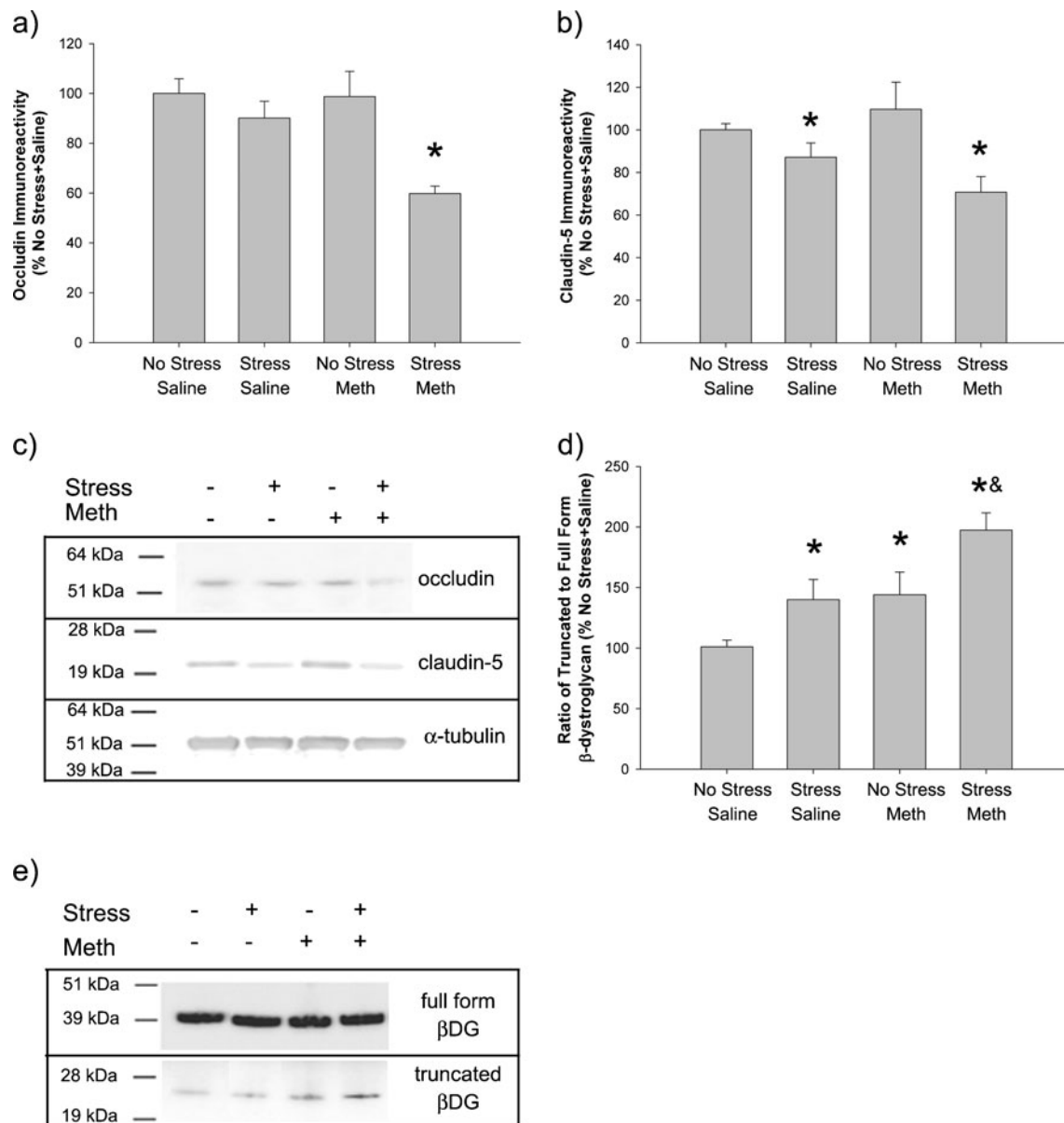
Fig. 2 Alterations in BBB structural proteins 24 hrs after treatment. Meth or saline was administered to previously stressed or control rats. Occludin and claudin-5 protein expression was measured in isolated brain capillaries via Western Blot. **a**) The combination of stress and Meth significantly decreased occludin immunoreactivity (*, $p<0.01$, compared to Stress + Saline and No Stress + Meth) ($n=8$–11 in each group) **b**) Exposure to stress significantly decreased claudin-5 immunoreactivity (*, $p=0.01$, compared to No Stress treated groups). ($n=8$–11 in each group) **c**) Representative Western Blot images illustrating occludin (57 kDa), claudin-5 (22 kDa) and α-tubulin (50 kDa) immunoreactive bands. **d**) Stress and Meth increased truncation of β-dystroglycan, compared to No Stress + Saline (*, $p<0.05$) and Stress + Meth significantly enhanced truncation of β-dystroglycan compared to No Stress + Meth and Stress + Saline (&, $p<0.001$). ($n=5$–7 in each group) **e**) Representative Western Blot images illustrating full-form (40 kDa) and truncated β-dystroglycan (22 kDa) immunoreactive bands

Figure 2b illustrates the quantification of claudin-5 protein expression in isolated capillaries and Fig. 2c is a representative Western Blot image of claudin-5 (22 kDa) and the loading control, α-tubulin (50 kDa). Stress significantly decreased claudin-5 protein expression (13 ±7 % decrease in the Stress + Saline treatment group and 29±7 % decrease in the Stress + Meth treatment group, compared to No Stress + Saline) as noted by a significant main effect of stress ($F_{1,35}=7.49$, $p=0.01$).

Figure 2d illustrates truncation of β-dystroglycan, as measured by the ratio of truncated (30 kDa) to full form (43 kDa) β-dystroglycan, 24 hrs after drug treatment. The combination of stress and Meth significantly increased the truncation of β-dystroglycan compared to all other

treatments, such that Stress + Saline produced a 40 ± 14 % increase, No Stress + Meth produced a 44 ± 19 % increase, and Stress + Meth produced a 97 ± 14 % increase compared to No Stress + Saline controls. These effects were revealed by a significant main effect of stress ($F_{1,24}=9.61$, $p<0.01$) and Meth ($F_{1,24}=11.37$, $p<0.01$). In addition, the Stress + Meth group was significantly different from No Stress + Meth ($t=-2.41$, $p<0.05$) and Stress + Saline groups ($t=-2.54$, $p<0.05$). Figure 2e is a representative Western Blot image of full form (43 kDa) and truncated (30 kDa) β-dystroglycan.

Effects of stress and meth on acute increases in brain water content

Figure 3 illustrates brain water content at 24 hrs after treatment. The combination of stress and Meth increased brain water content compared to No Stress + Saline treatment (81 ± 0.3 % water in the Stress + Meth versus 79 ± 0.2 % water in the No Stress + Saline group). A significant two-way interaction of stress and Meth ($F_{1,37}=11.07$, $p<0.01$) on brain water content was due to a significant increase in brain water content in the Stress + Meth group compared to the No Stress + Meth and Stress + Saline groups ($q=6.85$ and $q=5.76$; $p<0.001$, respectively). However, Stress + Saline and No Stress + Meth did not differ from No Stress + Saline treated rats.

Effects of stress and meth on acute alterations of FITC-dextran extravasation

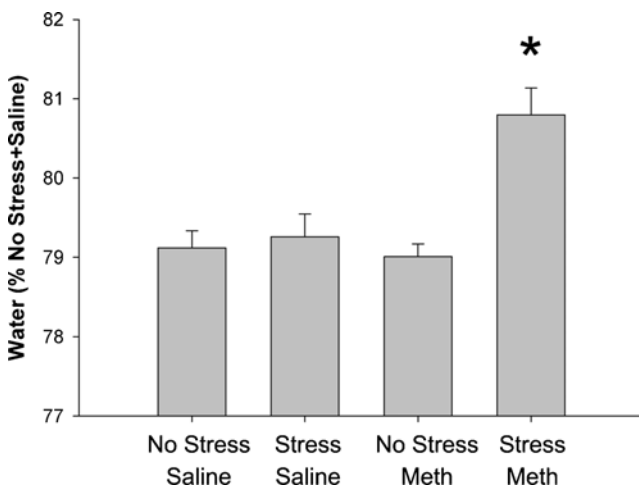FITC-dextran extravasation was used as a measure of BBB permeability. Figure 4a–f are representative images of

Fig. 3 Changes in brain water content, 24 hrs after treatment. Meth or saline was administered to previously stressed or control rats. The combination of stress and Meth significantly increased brain water content, compared to all other groups (*, $p<0.01$). ($n=8$–12 in each group)

cortical slices taken from rats perfused with FITC labeled dextran. While the saline treated groups as well as the No Stress + Meth treated group had distinct, brightly green stained capillaries against a black background, the Stress + Meth treatment resulted in a brighter green fluorescence in tissue surrounding and between the capillaries. In addition, areas of distinct leakage were apparent in the Stress + Meth group only, as illustrated in the inset images, 4E& 4F.

FITC-dextran extravasation in images from the cortex was quantified and illustrated in Fig. 4g. The combination of stress and Meth increased FITC-dextran extravasation by 231 ± 18 % in the cortex, compared to the No Stress + Saline control group. There was a significant effect of stress ($F_{1,11}=9.18$, $p<0.05$), Meth ($F_{1,11}=20.13$, $p<0.01$) and a significant interaction of stress and Meth ($F_{1,11}=6.93$, $p<0.05$) due primarily to a increase in FITC-dextran extravasation after Stress + Meth compared to No Stress + Meth ($q=5.66$; $p<0.001$) and Stress + Saline ($q=7.12$; $p<0.01$). There was no effect of stress on saline treated rats or an effect of Meth in the absence of stress.

It is important to note that the effects of stress and Meth on FITC-dextran extravasation were not brain region specific. Similar effects were observed in various regions of the cortex as well as the hippocampus and striatum (data not shown). To further validate the FITC-dextran experiments, brain areas lacking a BBB, such as the hypothalamus were evaluated. The hypothalamus had more FITC-dextran extravasation than brain regions that have a functional BBB, such as the cortex, hippocampus and striatum of control rats (data not shown).

Effects of stress and meth on acute neuroinflammation

Figure 5a illustrates the quantification of GFAP immunoreactivity at 24 hr after treatment. Figure 5b is a representative Western Blot image of GFAP (50 kDa) and α-tubulin (50 kDa). A two-way ANOVA did not reveal any significant effect of stress, Meth or the combination of stress and Meth on GFAP immunoreactivity in the cortex, 24 hr after treatment.

Figure 5c illustrates the quantification of COX-2 immunoreactivity at 24 hr after treatment. Figure 5d is a representative Western Blot image of COX-2 (72 kDa) and α-tubulin (50 kDa). There was no significant effect of stress, Meth or the combination of stress and Meth on COX-2 immunoreactivity at 24 hr in the cortex.

Effects of stress and meth on long-term neuroinflammation

Figure 6a illustrates the quantification of GFAP immunoreactivity, in cortical homogenate, 7 days after treatment. Figure 6b is a representative Western Blot image of GFAP
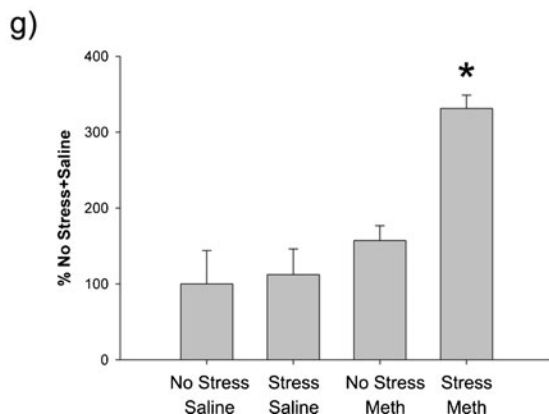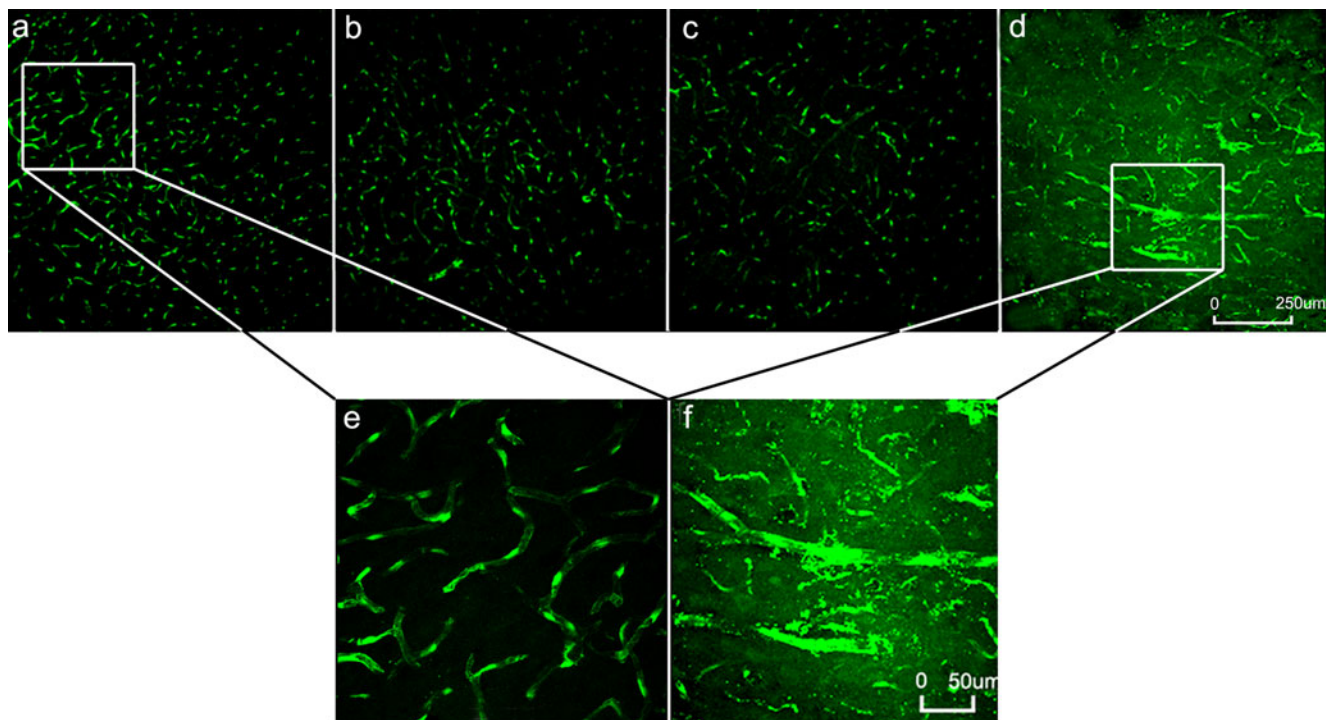
Fig. 4 Alterations in BBB permeability to FITC-dextran, 24 hrs after treatment. Meth or saline was administered to previously stressed or control rats. Extravasation of 10,000 dalton FITC-dextran was assessed 24 hrs after treatment. **a–f**) Representative 20× images of FITC-dextran in the cortex illustrate brightly green stained capillaries against a black background in the **a**) No Stress + Saline, **b**) Stress + Saline and **c**) No Stress + Meth treated groups, and brighter green fluorescence in tissue adjacent to the capillaries in the **d**) Stress + Meth group (scale bar: 250 μm). **e–f**) The inset figures illustrate areas of distinct leakage that were apparent in the **f**) Stress + Meth group only (scale bar: 50 μm). **g**) Quantification of FITC-dextran extravasation in the cortex, 24 hrs after treatment. The combination of stress and Meth significantly increased FITC-dextran extravasation in the cortex compared to all other groups (*, $p < 0.05$). ($n = 3$ in each group)

(50 kDa) and α-tubulin (50 kDa). Stress + Meth increased GFAP immunoreactivity in the cortex by 35 ± 8 %, compared to No Stress + Saline controls. There was a significant effect of Meth ($F_{1,24} = 5.04$, $p < 0.05$) and a significant interaction of stress and Meth ($F_{1,24} = 5.80$, $p < 0.05$). Post-hoc analysis indicated that Stress + Meth was significantly different from No Stress + Meth ($q = 4.33$, $p < 0.01$) and Stress + Saline ($q = 4.681$, $p < 0.01$) treatment groups, while Stress + Saline and No Stress + Meth were not different from No Stress + Saline controls.

Figure 6c illustrates the quantification of COX-2 immunoreactivity, in the whole cortex, at 7 days after treatment. Figure 6d is a representative Western Blot image of COX-2 (72 kDa) and α-tubulin (50 kDa). Stress + Meth increased COX-2 immunoreactivity in the cortex by 37 ± 6 %, compared to No Stress + Saline controls. An evaluation of the significant effect of stress ($F_{1,24} = 8.58$, $p < 0.01$), Meth ($F_{1,24} = 9.13$, $p < 0.01$) and a significant interaction of stress and Meth ($F_{1,24} = 5.66$, $p < 0.05$) showed that Stress + Meth had
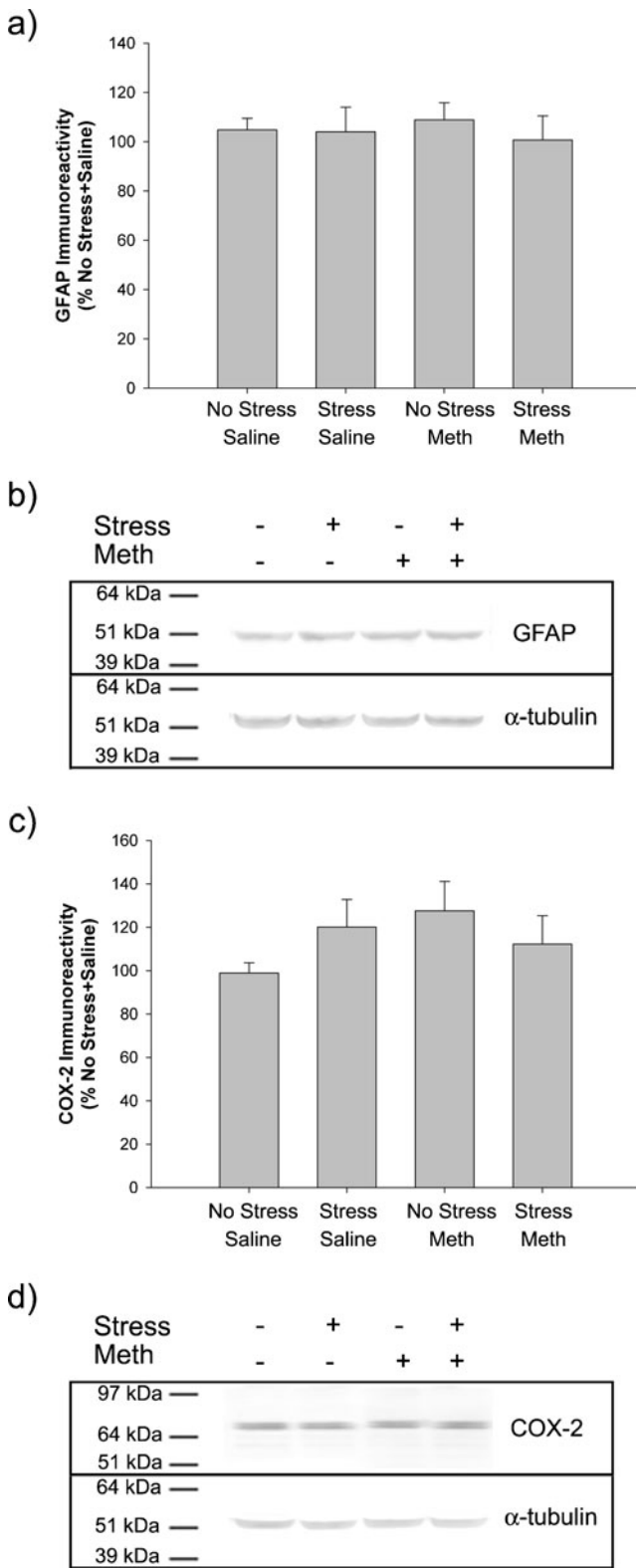
a)

b)

c)

d)

◄ Fig. 5 Markers of neuroinflammation, 24 hrs after treatment. Meth or saline was administered to previously stressed or control rats. GFAP and COX-2 protein expression was measured in cortex. **a**) GFAP immunoreactivity was not altered by stress or Meth. (n=6 in each group) **b**) Representative Western Blot images illustrating GFAP (50 kDa) and α-tubulin (50 kDa) immunoreactive bands. **c**) COX-2 immunoreactivity was not altered by stress or Meth. (n=6 in each group) **d**) Representative Western Blot images illustrating COX-2 (72 kDa) and α-tubulin (50 kDa) immunoreactive bands

Figure 7a illustrates the quantification of COX-2 immunoreactivity, in isolated cortical capillaries, 7 days after treatment. Figure 7b is a representative Western Blot image of COX-2 (72 kDa) and α-tubulin (50 kDa). In order to examine the effects of ketoprofen treatments on capillary COX-2 immunoreactivity in rats treated with the combination of stress and Meth, a one-way ANOVA with Bonferroni's post-hoc analysis was used to compare controls (all No Stress + Saline treated rats regardless of the type of ketoprofen treatment) with Stress + Meth, Stress + Meth + Ketoprofen-During &Post, Stress + Meth + Ketoprofen-During and Stress + Meth + Ketoprofen-Post treatment groups. Exposure to the combination of stress and Meth significantly increased COX-2 immunoreactivity in isolated capillaries by 42±6 % compared to controls (t=5.07, $p<$ 0.001). COX-2 immunoreactivity in the Stress + Meth + Ketoprofen-During & Post and Stress + Meth + Ketoprofen-Post treatment groups was significantly less than the Stress + Meth group (88±8 % and 98±6 % vs 144±6 %, respectively (t=5.02, $p<0.001$ and t=4.15, $p<0.01$)) and was not significantly different from the control group. In contrast, Stress + Meth + Ketoprofen-During treatment was not significantly different from Stress + Meth.

Effects of Ketoprofen on stress enhancement of meth-induced hyperthermia

The effects of Meth treatment, stress and ketoprofen on body temperatures are illustrated in Fig. 8. When body temperatures were measured 1 hr after each Meth or Saline injection, Meth administration (7.5 mg/kg ip × 4 every 2 hr), in previously stressed rats, produced a significant increase in core body temperatures of ~2 °C, compared to saline treated controls. These effects were revealed by a significant effect of treatment over time ($F_{16,304}$=12.34, $p<0.001$). Ketoprofen (5 mg/kg) administered during, after, or both during and after METH or saline injections, had no effect on hyperthermia.

Effects of Ketoprofen on stress and meth-induced persistent alterations of BBB transmembrane structural proteins

Figure 9a illustrates the quantification of occludin protein immunoreactivity in isolated capillaries. Figure 9c is a representative Western Blot image of occludin (57 kDa) and α-

significantly greater COX-2 expression than No Stress + Meth (q=5.28 $p<0.001$) and Stress + Saline (q=5.12, $p<0.01$) treatment groups, but Stress + Saline and No Stress + Meth groups did not differ from No Stress + Saline controls.
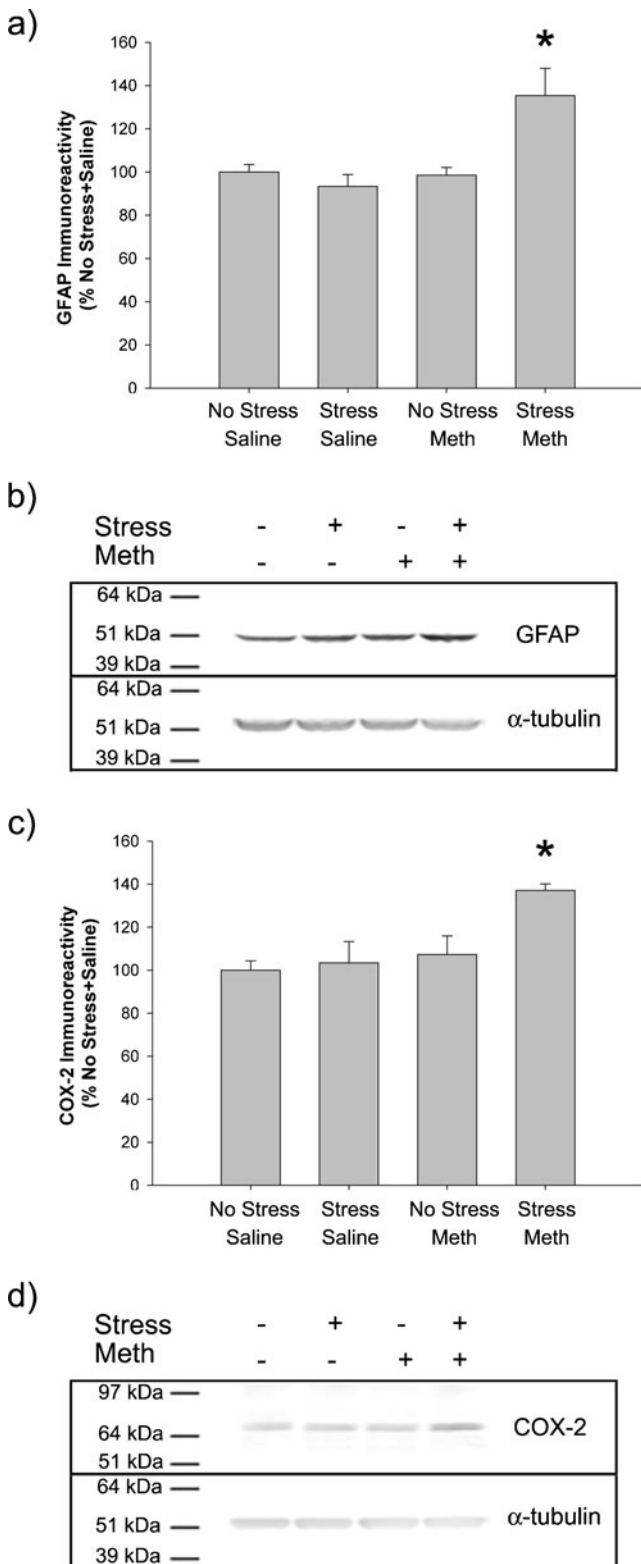
a)

b)

c)

d)

◀ **Fig. 6** Markers of neuroinflammation, 7 days after treatment. Meth or saline was administered to previously stressed or control rats. GFAP and COX-2 protein expression was measured in cortex. **a)** GFAP immunoreactivity was significantly increased by the combination of stress and Meth compared to all other groups (*, $p<0.05$). ($n=5$–8 in each group) **b)** Representative Western Blot images illustrating GFAP (50 kDa) and α-tubulin (50 kDa) immunoreactive bands. **c)** COX-2 immunoreactivity was significantly increased by the combination of stress and Meth compared to all other groups (*, $p<0.05$). ($n=5$–8 in each group) **d)** Representative Western Blot images illustrating COX-2 (72 kDa) and α-tubulin (50 kDa) immunoreactive bands

Saline treated rats regardless of the type of ketoprofen treatment) with Stress + Meth, Stress + Meth + Ketoprofen-During & Post treatment, Stress + Meth + Ketoprofen-During treatment and Stress + Meth + Ketoprofen-Post treatment. The combination of stress and Meth significantly decreased occludin immunoreactivity by
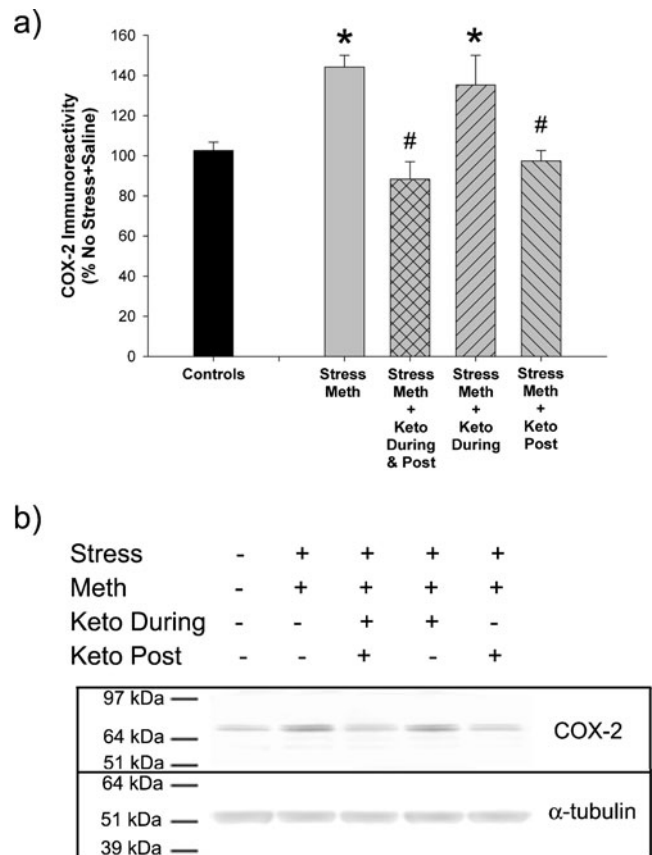

a)

b)

Fig. 7 COX-2 protein expression in isolated brain capillaries, 7 days after treatment. Meth or saline was administered to previously stressed or control rats. Ketoprofen was administered to some animals during, after or during and after the Meth or saline treatment. COX-2 protein expression was measured in isolated capillaries. **a)** COX-2 immunoreactivity was significantly increased by the combination of stress and Meth compared to Controls (No Stress + Saline treated rats regardless of ketoprofen treatment) (*, $p<0.001$). COX-2 increases were prevented when ketoprofen was administered during and after (#, $p<0.001$) or after Stress + Meth (#, $p<0.001$). ($n=6$–12 for all Stress + Meth groups, $n=19$ for Controls) **b)** Representative Western Blot images illustrating COX-2 (72 kDa) and α-tubulin (50 kDa) immunoreactive bands

tubulin (50 kDa). In order to examine the effects of ketoprofen treatments on occludin immunoreactivity in rats treated with the combination of stress and Meth, 7 days after treatment, a one-way ANOVA with Bonferroni's post-hoc analysis was used to compare controls (all No Stress +
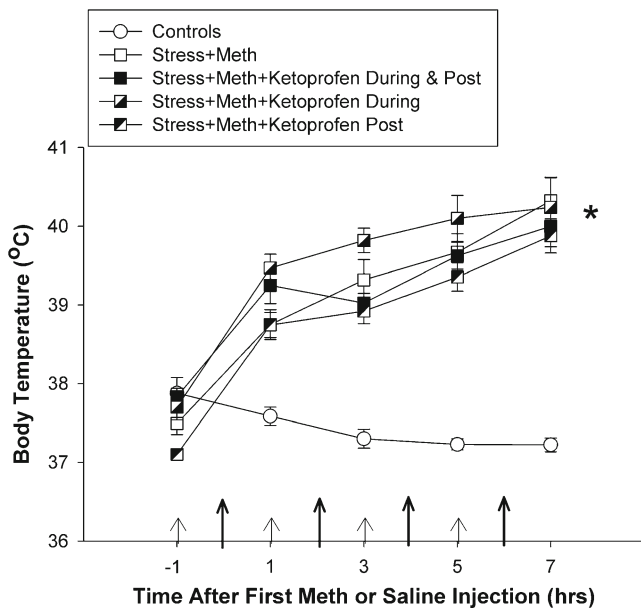
Fig. 8 Rectal temperatures after exposure to stress, Meth and ketoprofen. Meth or saline was administered to previously stressed or control rats. Some rats received ketoprofen 1 hr before each Meth or saline injection (Ketoprofen During). Those rats that received ketoprofen post-treatment only, have not yet been exposed to ketoprofen. Body temperatures were measured before and every hr after a Meth or saline injection. Larger arrows on the x-axis indicate the time of Meth or saline injections. The smaller arrows indicate ketoprofen or vehicle injections. The combination of stress and Meth significantly increased body temperature over time (*, $p < 0.001$) and ketoprofen had no effect on Stress + Meth-induced hyperthermia. ($n = 9$–16 in each group)

42±7 %, compared to the control group ($t = 4.48$, $p < 0.001$). The Stress + Meth + Ketoprofen-During treatment was also significantly different from the control group (Stress + Meth + Ketoprofen-During, 58±9 % vs control, 99±3 %, $t = 3.80$, $p < 0.01$), but was not significantly different from the Stress + Meth group. The Stress + Meth + Ketoprofen-During & Post treatment group and Stress + Meth + Ketoprofen-Post treatment group, however, were significantly different from the Stress + Meth group (Stress + Meth + Ketoprofen During & Post, 106±12 % vs Stress + Meth, 57±7 %, $t = 4.60$, $p < 0.001$; Stress + Meth + Ketoprofen Post, 101±12 % vs Stress + Meth, 57±7 %, $t = 3.43$, $p < 0.05$), but not the control group.

Figure 9b illustrates the quantification of claudin-5 immunoreactivity in isolated capillaries. Figure 9c is a representative Western Blot image of claudin-5 (22 kDa) and α-tubulin (50 kDa). To examine the effects of ketoprofen treatments on claudin-5 immunoreactivity, 7 days after treatment, in rats treated with the combination of stress and Meth, a one-way ANOVA with Bonferroni's post-hoc analysis was used to compare controls (all No Stress + Saline treated rats regardless of the type of ketoprofen treatment) with Stress + Meth, Stress + Meth + Ketoprofen-During & Post treatment, Stress + Meth + Ketoprofen-During treatment and Stress + Meth + Ketoprofen-Post treatment
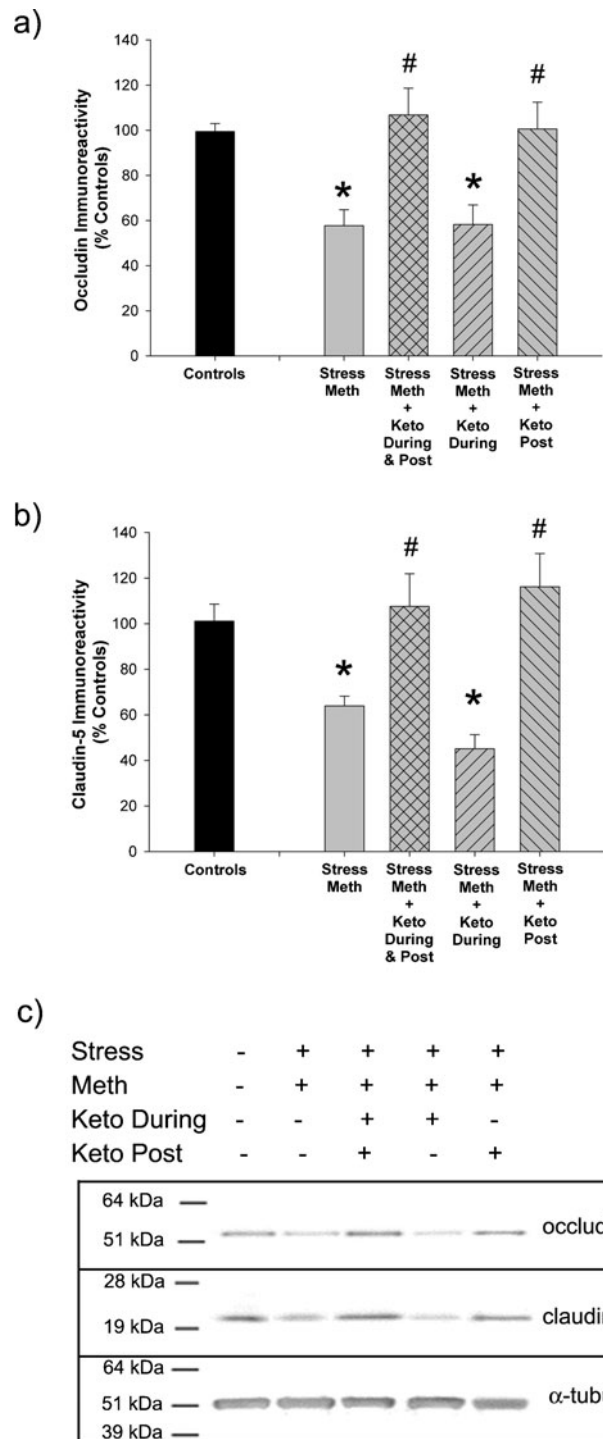

Fig. 9 Long-term alterations in BBB transmembrane structural proteins, 7 days after treatment. Meth or saline was administered to previously stressed or control rats. Some rats received ketoprofen during, after or during and after the Meth or saline treatment. Occludin and claudin-5 protein expression was assessed 7 days after treatment. Stress + Meth significantly decreased **a**) occludin and **b**) claudin-5 immunoreactivity and ketoprofen administered during and after or after treatment prevented the occludin decreases (*, $p < 0.01$, compared to Controls; #, $p < 0.05$, compared to Stress + Meth). ($n = 7$–16 in each group) **c**) Representative Western Blot images illustrating occludin (57 kDa), claudin-5 (22 kDa) and α-tubulin (50 kDa) immunoreactive bands

groups. The combination of stress and Meth produced a significant 37 ± 4 % decrease in claudin-5 protein expression, compared to controls ($t=3.55$, $p<0.01$). The Stress + Meth + Ketoprofen-During treatment was also significantly different from the control group (Stress + Meth + Ketoprofen-During, 58 ± 9 % vs control, 99 ± 3 %, $t=4.37$, $p<0.001$), but was not significantly different from the Stress + Meth group. The Stress + Meth + Ketoprofen During & Post treatment group and Stress + Meth + Ketoprofen-Post treatment group, however, were significantly different from the Stress + Meth group (Stress + Meth + Ketoprofen-During & Post, 107 ± 14 % vs Stress + Meth, 63 ± 4 %, $t=3.51$, $p<0.01$; Stress + Meth + Ketoprofen-Post, 116 ± 15 % vs Stress + Meth, 63 ± 4 %, $t=3.69$, $p<0.05$), but did not differ from controls.

There was no effect of the combination of stress and Meth on truncation of β-dystroglycan, 7 days after treatment (data not shown).

Effects of Ketoprofen on stress and meth-induced persistent increases in brain water content

Brain water content was not altered by the combination of stress and Meth, 7 days after treatment (data not shown).

Effects of Ketoprofen on stress and meth-induced persistent alterations of FITC-dextran extravasation

On the 7th day after treatment, FITC labeled dextran was intracardially perfused to observe the long-term effects of stress and Meth on BBB permeability. Figures 10a–e are representative images of cortical slices taken from rats perfused with FITC labeled dextran 7 days after the administration of Meth or saline. The Stress + Meth and Stress + Meth + Ketoprofen-During treatment groups had brighter green fluorescence in the tissue surrounding and between the capillaries compared to all other treatment groups. It was also noted that the No Stress + Saline treated groups, the Stress + Meth + Ketoprofen-During & Post treated group and the Stress + Meth + Ketoprofen Post-treated group showed green fluorescence restricted to the capillaries and not in the surrounding tissue.

The extravasation of FITC-dextran in cortical images was quantified and the results are illustrated in Fig. 10f. To examine the effects of ketoprofen treatments on FITC-dextran extravasation in rats treated with the combination of stress and Meth, a one-way ANOVA with Bonferroni's post-hoc analysis was used to compare controls (all No Stress + Saline treated rats regardless of the type of ketoprofen treatment), Stress + Meth, Stress + Meth + Ketoprofen-During & Post, Stress + Meth + Ketoprofen-During and Stress + Meth + Ketoprofen-Post treatment groups. The combination of stress and Meth produced a

significant 178 ± 42 % increase in FITC-dextran extravasation in the cortex, compared to controls ($t=4.04$, $p<0.05$). The measures of FITC-dextran extravasation, in the Stress + Meth + Ketoprofen-During & Post and Stress + Meth + Ketoprofen-Post treatment groups were significantly less than the Stress + Meth treatment group (Stress + Meth + Ketoprofen-During & Post, 81 ± 23 % vs Stress + Meth, 278 ± 42 %, $t=3.85$, $p<0.05$; Stress + Meth + Ketoprofen-Post, 102 ± 24 % vs Stress + Meth, 278 ± 42 %, $t=3.44$, $p<0.05$), but the Stress + Meth + Ketoprofen-During treated groups did not differ from the Stress + Meth treated group.

Effects of the prostaglandin EP1 receptor antagonist, SC-51089, on stress and meth-induced persistent alterations of FITC-dextran extravasation

Figures 11a–d illustrate representative images of cortical slices taken from rats perfused with FITC labeled dextran 7 days after the exposure to Stress + Meth or No Stress + Saline and post-treated with 10 μg/kg SC-51089 or 0.02 % DMSO, twice a day every day after Meth or saline treatments. While the No Stress + Saline treated groups and the Stress + Meth + SC-51089 Post treated group had brightly green stained capillaries against a black background, the Stress + Meth treatment group had brighter green fluorescence in the tissue surrounding and between the capillaries.

The extravasation of FITC-dextran in cortical images was quantified and the results are illustrated in Fig. 11e. There was a significant effect of Stress + Meth treatment ($F_{1,13}=13.39$, $p<0.01$) and a significant interaction of Stress + Meth and SC-51089 post-treatment ($F_{1,13}=4.98$, $p<0.05$). Further evaluation showed that Stress + Meth produced a significant 184 ± 33 % increase in FITC-dextran, compared to No Stress + Saline controls ($q=5.59$, $p<0.01$) and SC-51089 treatments (Stress + Meth + SC-51089) blocked the increase in FITC-dextran extravasation produced by Stress + Meth (162 ± 26 % vs 284 ± 33 %, respectively; $q=4.16$, $p<0.05$).

Discussion

The role of neuroinflammation in the acute and long-term alterations in BBB structure and function resulting from serial exposure to stress and Meth was investigated. Serial exposure to stress and Meth decreased structural proteins of the BBB and increased BBB permeability within 24 hours that persisted up to 7 days after Meth treatment. While markers of neuroinflammation were not observed 24 hours after stress and/or Meth treatment, increases in GFAP and increased COX-2 expression in brain capillaries paralleled the BBB disruption observed at 7 days, after serial exposure
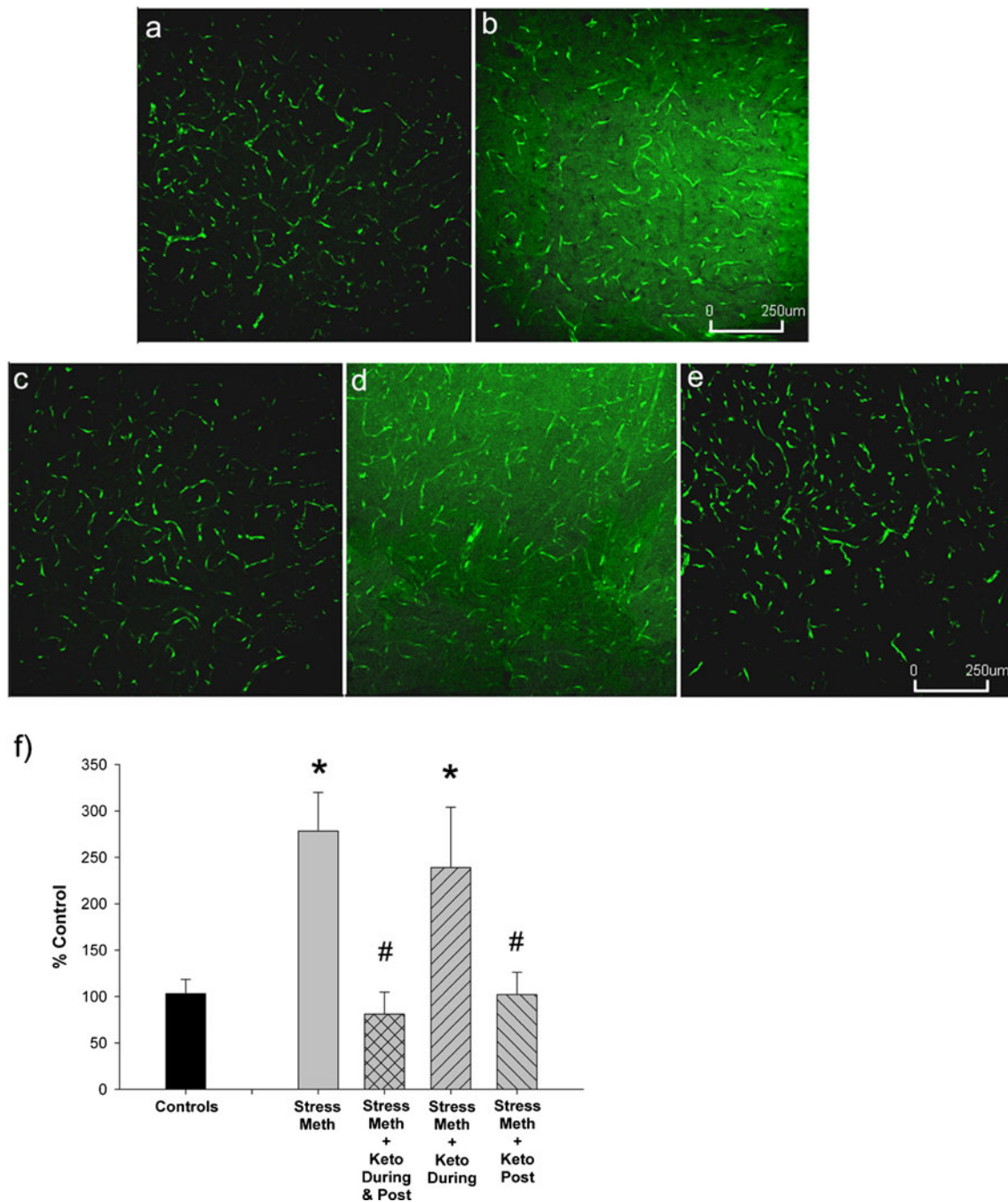
Fig. 10 Long-term alterations in BBB permeability to FITC-dextran, 7 days after treatment, are prevented by ketoprofen administration after treatment. Meth or saline was administered to previously stressed or control rats. Some rats received ketoprofen during, after or during and after the Meth or saline treatment. Extravasation of 10,000 dalton FITC-dextran was assessed 7 days after treatment. a–e) Representative 20× images of FITC-dextran in the cortex illustrate brightly green stained capillaries against a black background in the a) Control, c) Stress + Meth + Ketoprofen During & Post treatment, and e) Stress + Meth + Ketoprofen Post treatment, while there was a brighter green fluorescence in tissue adjacent to the capillaries in the b) Stress + Meth and d) Stress + Meth + Ketoprofen During treatment groups. (scale bar: 250 μm) f) Quantification of FITC-dextran extravasation in the cortex, 7 days after treatment. The combination of stress and Meth significantly increased FITC-dextran extravasation in the cortex compared to Controls and this increase was prevented by ketoprofen administered during and after or after treatment (*, $p < 0.01$, compared to Controls; #, $p < 0.05$, compared to Stress + Meth). ($n = 3$ in each group)

to stress and Meth. In addition, persistent increases in BBB permeability were prevented by the inhibition of COX and the antagonism of the prostaglandin PGE2 EP1 receptor.

Serial exposure to stress and Meth acutely decreased the expression of tight junction proteins, occludin and claudin-5, in isolated cortical capillaries within 24 hours (Fig. 2).

Fig. 11 Long-term alterations in BBB permeability to FITC-dextran, 7 days after treatment, are prevented by SC-51089 administration after treatment. Meth or saline was administered to previously stressed or control rats. Some rats received SC-51089 twice a day for 6 days after Meth or saline treatment. Extravasation of 10,000 dalton FITC-dextran was assessed 7 days after treatment. **a–d**) Representative 20× images of FITC-dextran in the cortex illustrate brightly green stained capillaries against a black background in the **a**) No Stress + Saline + Vehicle, **c**) No Stress + Saline + SC-51089 and **d**) Stress + Meth + SC-51089, while there was a brighter green fluorescence in tissue adjacent to the capillaries in the **b**) Stress + Meth + Vehicle treated group. (scale bar: 250 μm) f) Quantification of FITC-dextran extravasation in the cortex, 7 days after treatment. The combination of stress and Meth significantly increased FITC-dextran extravasation in the cortex compared to No Stress + Saline + Vehicle (*, $p<0.01$) and this increase was prevented by SC-51089 post-treatment (#, $p< 0.05$, compared to Stress + Meth). ($n=3–4$ in each group)
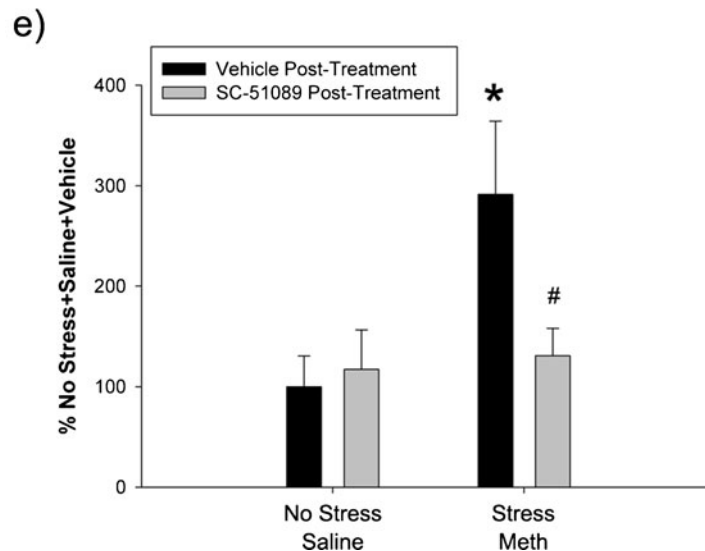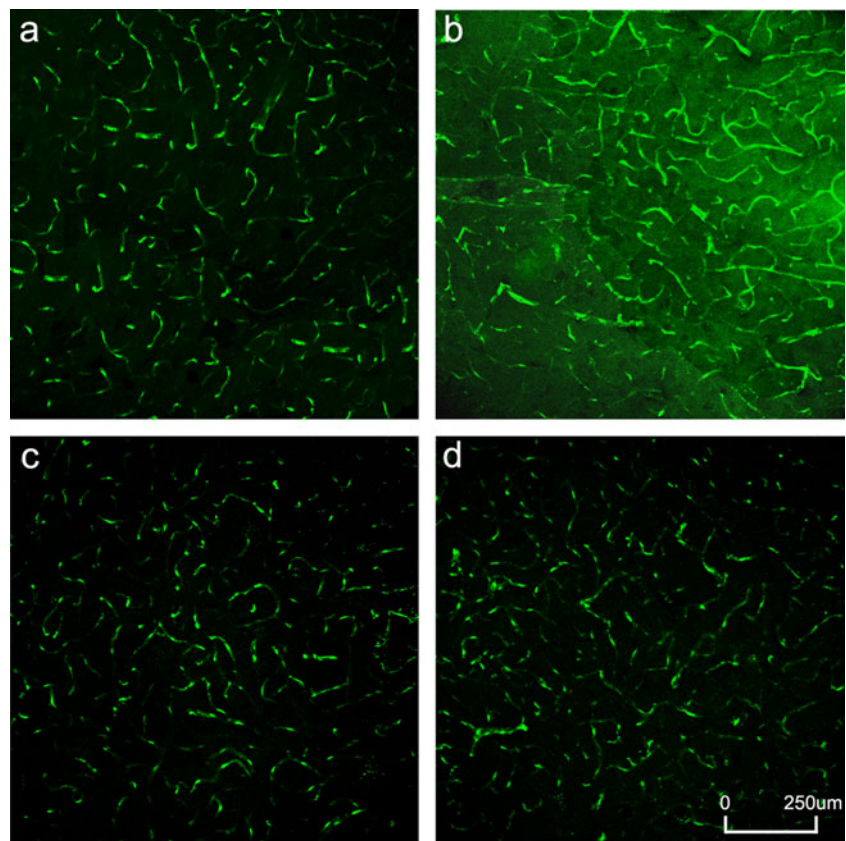
These changes also coincided with an increase in FITC-dextran fluorescence in tissue surrounding the capillaries (Fig. 4) in rats exposed to the combination of stress and Meth. The increase in dextran extravasation is indicative of an increase in BBB permeability that is likely reflective of the collective decreases in tight junction proteins. While Meth alone had no effect on BBB structure or function, CUS itself decreased claudin-5. The mechanism for this selective effect is unclear, but the decrease in claudin-5 after

CUS alone was insufficient to increase BBB permeability or edema (Fig. 4). This is consistent with previous findings that claudin-5 knockout mice do not exhibit brain edema and increased permeability to molecules greater than 800 Da (Nitta et al. 2003). Although others have observed a transient disruption of the BBB in response to high doses of Meth (Bowyer and Ali 2006; Kiyatkin et al. 2007; Kiyatkin and Sharma 2009b; Kousik et al. 2011; Martins et al. 2011; Park et al. 2012), these data are the first to indicate that

stress and a moderate dose of Meth synergize to cause structural and functional disruptions of the BBB.

The lack of effect of Meth alone on BBB disruption may be due to the moderate dose of Meth used in these studies. In the majority of studies that observe Meth-induced BBB disruption at 24 hrs in areas of the cortex, hippocampus and striatum, a single high bolus dose of 30–40 mg/kg Meth was administered (Bowyer and Ali 2006; Kiyatkin et al. 2007; Kiyatkin and Sharma 2009a). This dose is equal to or greater than the total of 30 mg/kg (7.5 mg/kg × 4) of Meth administered over a 6 hr period in the current study. A single dose of 30–40 mg/kg has been shown by Bowyer and Ali (2006) to produce extreme hyperthermia and seizures that correlated with the extent of Meth-induced hyperthermia and duration of status epilepticus. A study by Kiyatkin et al. (2007) reported that 9 mg/kg administered in an ambient temperature of 29 °C produced a 2 °C increase in brain temperature and BBB permeability in the cortex. In the current experiments, our dosing regimen only produced an increase in body temperature of only about 1 °C (Fig. 1) and did not produce seizures. Taken together, these data suggest that Meth-induced hyperthermia is a major contributor to the early and acute BBB disruption caused by Meth alone. It is interesting to note though that Meth administered at a dose of 7.5 mg/kg i.p. q 2 hr × 4 does produce slight depletions in monoamines in the striatum (Tata et al. 2007), but does not produce BBB disruption. While the reason for the differential effect of Meth on monoamine terminals and the BBB is unknown, it is clear that the mechanisms of monoaminergic damage and BBB damage, in response to Meth alone, differ such that early BBB damage is not required for long-term monoamine depletions.

While the mechanisms by which stress potentiates Meth-induced BBB disruption at early time points was not investigated in the present study, the enhanced BBB disruption may be due to enhanced hyperthermia (Fig. 1). Stress potentiates Meth-induced hyperthermia (Fig. 1) and Bowyer and Ali (2006) and Kiyatkin et al. (2007) have suggested that the transient BBB disruption caused by high-dose Meth is highly correlated with the degree of hyperthermia. Alternatively, stress and Meth may mediate early BBB disruption through increased oxidative stress and inflammatory cytokines. In fact, stress and Meth produce oxidative stress (Yamamoto and Zhu 1998; Madrigal et al. 2001), which contributes to BBB disruption and brain edema after acute ischemia-reperfusion (Mohammadi et al. 2011). Additionally, stress and Meth independently increase the production of pro-inflammatory cytokines (Flora et al. 2002; Garcia-Bueno et al. 2008; Loftis et al. 2011) in the brain that in turn are known to mediate BBB disruption after ischemia (Yang et al. 1999) or streptococcus agalactiae infection (Barichello et al. 2011). Therefore, hyperthermia, oxidative stress and cytokines may work in concert to produce the early BBB alterations in response to stress and Meth.

Increases in brain water content (Fig. 3) were also evident at 24 hours after serial exposure to stress and Meth, indicative of vasogenic or cytotoxic edema. The observed vasogenic-like edema is the likely consequence of the concomitant decreases in tight junction proteins (Fig. 2). Moreover, the truncation of full length β-dystroglycan may be indicative of the breakdown of the hydrophobic barrier that is normally formed by β-dystroglycan, which crosslinks astrocytic endfeet and endothelial cells with the basal lamina (Fig. 2). β-dystroglycan also regulates aquaporin 4 (AQP4) localization, which is typically localized to astrocytic endfeet and participates in clearing extracellular fluid from the brain parenchyma during vasogenic edema (Papadopoulos et al. 2004). Therefore, loss or truncation of β-dystroglycan could result in the loss of the polarized localization of AQP4 in astrocytic endfeet (Wolburg-Buchholz et al. 2009) and exacerbate edema. However, when measured one week after Meth, β-dystroglycan and water content were unaltered (data not shown). The lack of long-term damage to β-dystroglycan may be due to the high turnover rate of β-dystroglycan (Michaluk et al. 2007). Regardless, the absence of truncated β-dystroglycan coincides with the lack of edema at 7 days whereas the presence of β-dystroglycan truncation may be partially responsible for edema at 24 hours.

Some of the other structural and functional disruptions of the BBB observed in response to serial exposure to stress and Meth, including decreases in tight junction proteins (Fig. 9) and increases in FITC-dextran extravasation (Fig. 10), were persistent and paralleled by long-term neuroinflammation. The longer lasting neuroinflammation resulting from serial exposure to stress and Meth, compared to stress or Meth alone, may be due to preexisting neuroinflammation produced by stress (Nair and Bonneau 2006; Garcia-Bueno et al. 2008) that synergizes with the neuroinflammatory effects of Meth (Thomas et al. 2004; Thomas and Kuhn 2005; Loftis et al. 2011). In fact, preexisting neuroinflammation increases the vulnerability of the brain to subsequent neuroinflammatory events (Johnson et al. 2002; Perry 2007). Thus, Meth administration could enhance and/or prolong neuroinflammation after stress that leads eventually to disruption of the BBB.

GFAP immunoreactivity was increased 7 days after exposure to the combination of stress and Meth, but not to stress or Meth alone (Fig. 6), indicating an increased reactivity of astrocytes that surround the capillaries. It is unclear whether the increases in GFAP are a cause or a response to the BBB damage caused by the combination of stress and Meth. Although glial activation and neuroinflammation exacerbate neurotoxicity, neuroinflammation can also be a reparative mechanism (Hirsch et al. 2003; Verkhratsky et al. 2010). In particular, astrocytes increase the integrity of BBB (Dehouck et al. 1990) and may assist in the repair of BBB damage. While the stress and Meth-induced increases

in GFAP may be compensatory mechanisms to repair a damaged BBB, there is no evidence of recovery at 7 days, despite the observed increased GFAP immunoreactivity. Whether the recovery from BBB damage occurs some time after the observed increases in GFAP at 7 days remains to be determined.

COX-2 immunoreactivity was also increased 7 days after the exposure to the combination of stress and Meth (Fig. 6) and subsequently determined to be localized to the brain endothelial cells (Fig. 7). This finding that stress and Meth increase COX-2 expression in brain endothelial cells of the rat is in agreement with the finding that Meth can induce AP-1 and NFKB in human brain endothelial cells in culture (Lee et al. 2001). Collectively, these data indicate endothelial cells can respond to insults and produce inflammatory mediators such as COX-2 that can cause damage to the BBB.

Increased COX activity has been associated with BBB disruption in response to ischemia and TBI and, therefore, it was hypothesized that the persistent increases in COX-2, mediate the long-lasting BBB disruption observed in response to the serial exposure to stress and Meth. The long-term structural and functional BBB disruptions were prevented only when ketoprofen was administered for the 7 days after combined exposure to stress and Meth. When ketoprofen treatment was limited only to the time coincident with Meth exposure, no mitigating effect on neuroinflammation or long-term BBB disruption was observed. In contrast, ketoprofen administered every day after treatment prevented the disruption of BBB structure (Fig. 9) and function (Fig. 10) as well as the sustained increases in COX-2 immunoreactivity in brain endothelial cells (Fig. 7). Moreover, the protective effects of ketoprofen on the long-lasting BBB alterations produced by the serial exposure to stress and Meth are due to inhibition of COX activity rather than attenuation of hyperthermia (Fig. 8). The lack of modulation of Meth-induced hyperthermia and BBB disruption by ketoprofen, when administered during Meth, suggests that COX and prostaglandin activity do not mediate Meth-induced hyperthermia. Therefore, the acute increases in COX activity and hyperthermia during Meth treatment are not responsible for the long-term BBB disruption observed after serial exposure to stress and Meth. When the same dose of ketoprofen was administered after but not during Meth treatment, the long-term BBB disruption was prevented. This result indicates that the combination of stress and Meth produces a delayed and prolonged state of COX-mediated neuroinflammation to cause a persistent disruption of the BBB.

COX activity may mediate BBB disruption through downstream activation of the prostaglandin PGE_2, EP1 receptor (Fukumoto et al. 2010) and activation of matrix metalloproteases (MMPs) (Candelario-Jalil et al. 2007; Aid et al. 2010). Data illustrated in Fig. 11, suggests that the EP1 receptor is involved in the long-lasting BBB disruption observed in response to serial exposure to stress and Meth, as the EP1 receptor antagonist, SC-51089, attenuated the increases in BBB permeability (Fig. 11). While the role of EP1 receptor activation in disruption of BBB structures was not investigated, EP1 receptor signaling can lead to activation of kinases (Bos et al. 2004) and subsequent phosphorylation and destruction of occludin and claudin-5 (Yamamoto et al. 2008). Nonetheless, the current data suggest that the mechanism of COX-dependent BBB damage is due partly to increased COX-2 activity in brain endothelial cells and subsequent activation of the EP1 receptor.

In conclusion, the results demonstrate that the scope of long-term damage produced by the serial exposure to stress and METH is broadened beyond damage to neurotransmitter systems and now includes long-term damage to the BBB. Importantly, these results indicate that stress can increase the vulnerability of the brain to a variety of insults and exacerbate those that produce neuroinflammation. Moreover, stress synergizes with Meth to produce long-lasting BBB disruption mediated by COX activity in endothelial cells, suggesting a long-lasting vulnerability of the brain to subsequent insults that could be attenuated with non-steroidal anti-inflammatory drug (NSAID) treatment. The observed long-lasting breach of the BBB may also contribute to the long-term neurodegeneration and cognitive deficits produced by Meth (Wagner et al. 1980; Chapman et al. 2001). Additional neurotoxicity may also occur with the added exposure to stress and produce increased extravasation of endogenous or exogenous neurotoxic proteins (e.g. HIV) and pro-inflammatory molecules. Moreover, damage to the BBB can also cause decreased transcellular transport activity from the brain to blood by endothelial cells resulting in the accumulation of waste products (Quaegebeur et al. 2011). Therefore, the synergistic neuroinflammatory interactions between stress and Meth illustrate that chronic stress could damage the BBB in the presence of non-toxic doses of Meth or conversely, non-toxic doses of Meth would be rendered toxic by chronic stress.

Conflict of interest The authors declare that they have no conflict of interest.

References

Abbott NJ (2000) Inflammatory mediators and modulation of blood-brain barrier permeability. Cell Mol Neurobiol 20:131–147

Abdul Muneer PM, Alikunju S, Szlachetka AM, Murrin LC, Haorah J (2011) Impairment of brain endothelial glucose transporter by methamphetamine causes blood-brain barrier dysfunction. Mol Neurodegener 6:23

Aid S, Silva AC, Candelario-Jalil E, Choi SH, Rosenberg GA, Bosetti F (2010) Cyclooxygenase-1 and -2 differentially modulate lipopolysaccharide-induced blood-brain barrier disruption through matrix metalloproteinase activity. J Cereb Blood Flow Metab 30:370–380

Asanuma M, Tsuji T, Miyazaki I, Miyoshi K, Ogawa N (2003) Methamphetamine-induced neurotoxicity in mouse brain is attenuated by ketoprofen, a non-steroidal anti-inflammatory drug. Neurosci Lett 352:13–16

Barichello T, Lemos JC, Generoso JS, Cipriano AL, Milioli GL, Marcelino DM, Vuolo F, Petronilho F, Dal-Pizzol F, Vilela MC, Teixeira AL (2011) Oxidative stress, cytokine/chemokine and disruption of blood–brain barrier in neonate rats after meningitis by streptococcus agalactiae. Neurochem Res

Bos CL, Richel DJ, Ritsema T, Peppelenbosch MP, Versteeg HH (2004) Prostanoids and prostanoid receptors in signal transduction. Int J Biochem Cell Biol 36:1187–1205

Bowyer JF, Ali S (2006) High doses of methamphetamine that cause disruption of the blood–brain barrier in limbic regions produce extensive neuronal degeneration in mouse hippocampus. Synapse 60:521–532

Candelario-Jalil E, Taheri S, Yang Y, Sood R, Grossetete M, Estrada EY, Fiebich BL, Rosenberg GA (2007) Cyclooxygenase inhibition limits blood–brain barrier disruption following intracerebral injection of tumor necrosis factor-alpha in the rat. J Pharmacol Exp Ther 323:488–498

Chapman DE, Hanson GR, Kesner RP, Keefe KA (2001) Long-term changes in basal ganglia function after a neurotoxic regimen of methamphetamine. J Pharmacol Exp Ther 296:520–527

Cruickshank CC, Dyer KR (2009) A review of the clinical pharmacology of methamphetamine. Addiction 104:1085–1099

Dehouck MP, Meresse S, Delorme P, Fruchart JC, Cecchelli R (1990) An easier, reproducible, and mass-production method to study the blood–brain barrier in vitro. J Neurochem 54:1798–1801

Ernst T, Chang L, Leonido-Yee M, Speck O (2000) Evidence for long-term neurotoxicity associated with methamphetamine abuse: A 1H MRS study. Neurology 54:1344–1349

Eyerman DJ, Yamamoto BK (2007) A rapid oxidation and persistent decrease in the vesicular monoamine transporter 2 after methamphetamine. J Neurochem 103:1219–1227

Flora G, Lee YW, Nath A, Maragos W, Hennig B, Toborek M (2002) Methamphetamine-induced TNF-alpha gene expression and activation of AP-1 in discrete regions of mouse brain: potential role of reactive oxygen intermediates and lipid peroxidation. Neuromolecular Med 2:71–85

Foster RT, Jamali F (1988) Stereoselective pharmacokinetics of ketoprofen in the rat. Influence of route of administration. Drug Metabol Dispos 16:623–626

Fukumoto K, Takagi N, Yamamoto R, Moriyama Y, Takeo S, Tanonaka K (2010) Prostanoid EP1 receptor antagonist reduces blood-brain barrier leakage after cerebral ischemia. Eur J Pharmacol 640:82–86

Garcia-Bueno B, Caso JR, Leza JC (2008) Stress as a neuroinflammatory condition in brain: damaging and protective mechanisms. Neurosci Biobehav Rev 32:1136–1151

Haile CN, GrandPre T, Kosten TA (2001) Chronic unpredictable stress, but not chronic predictable stress, enhances the sensitivity to the behavioral effects of cocaine in rats. Psychopharmacology 154:213–220

Hawkins BT, Abbruscato TJ, Egleton RD, Brown RC, Huber JD, Campos CR, Davis TP (2004) Nicotine increases in vivo blood-brain barrier permeability and alters cerebral microvascular tight junction protein distribution. Brain Res 1027:48–58

Hirsch EC, Breidert T, Rousselet E, Hunot S, Hartmann A, Michel PP (2003) The role of glial reaction and inflammation in Parkinson's disease. Ann N Y Acad Sci 991:214–228

Hotchkiss AJ, Gibb JW (1980) Long-term effects of multiple doses of methamphetamine on tryptophan hydroxylase and tyrosine hydroxylase activity in rat brain. J Pharmacol Exp Ther 214:257–262

Johnson BN, Yamamoto BK (2009) Chronic unpredictable stress augments +3,4-methylenedioxymethamphetamine-induced monoamine depletions: the role of corticosterone. Neuroscience 159:1233–1243

Johnson JD, O'Connor KA, Deak T, Stark M, Watkins LR, Maier SF (2002) Prior stressor exposure sensitizes LPS-induced cytokine production. Brain Behav Immun 16:461–476

Kawano T, Anrather J, Zhou P, Park L, Wang G, Frys KA, Kunz A, Cho S, Orio M, Iadecola C (2006) Prostaglandin E2 EP1 receptors: downstream effectors of COX-2 neurotoxicity. Nat Med 12:225–229

Kita T, Shimada K, Mastunari Y, Wagner GC, Kubo K, Nakashima T (2000) Methamphetamine-induced striatal dopamine neurotoxicity and cyclooxygenase-2 protein expression in BALB/c mice. Neuropharmacology 39:399–406

Kiyatkin EA, Sharma HS (2009a) Permeability of the blood-brain barrier depends on brain temperature. Neuroscience 161:926–939

Kiyatkin EA, Sharma HS (2009b) Acute methamphetamine intoxication brain hyperthermia, blood-brain barrier, brain edema, and morphological cell abnormalities. Int Rev Neurobiol 88:65–100

Kiyatkin EA, Brown PL, Sharma HS (2007) Brain edema and breakdown of the blood-brain barrier during methamphetamine intoxication: critical role of brain hyperthermia. Eur J Neurosci 26:1242–1253

Kousik SM, Graves SM, Napier TC, Zhao C, Carvey PM (2011) Methamphetamine-induced vascular changes lead to striatal hypoxia and dopamine reduction. Neuroreport 22:923–928

Lee YW, Hennig B, Yao J, Toborek M (2001) Methamphetamine induces AP-1 and NF-kappaB binding and transactivation in human brain endothelial cells. J Neurosci Res 66:583–591

Loftis JM, Choi D, Hoffman W, Huckans MS (2011) Methamphetamine causes persistent immune dysregulation: a cross-species, translational report. Neurotox Res 20:59–68

Madrigal JL, Olivenza R, Moro MA, Lizasoain I, Lorenzo P, Rodrigo J, Leza JC (2001) Glutathione depletion, lipid peroxidation and mitochondrial dysfunction are induced by chronic stress in rat brain. Neuropsychopharmacology 24:420–429

Madrigal JL, Moro MA, Lizasoain I, Lorenzo P, Fernandez AP, Rodrigo J, Bosca L, Leza JC (2003) Induction of cyclooxygenase-2 accounts for restraint stress-induced oxidative status in rat brain. Neuropsychopharmacology 28:1579–1588

Martins T, Baptista S, Goncalves J, Leal E, Milhazes N, Borges F, Ribeiro CF, Quintela O, Lendoiro E, Lopez-Rivadulla M, Ambrosio AF, Silva AP (2011) Methamphetamine transiently increases the blood-brain barrier permeability in the hippocampus: role of tight junction proteins and matrix metalloproteinase-9. Brain Res 1411:28–40

Matuszewich L, Yamamoto BK (2004) Chronic stress augments the long-term and acute effects of methamphetamine. Neuroscience 124:637–646

McCann UD, Wong DF, Yokoi F, Villemagne V, Dannals RF, Ricaurte GA (1998) Reduced striatal dopamine transporter density in abstinent methamphetamine and methcathinone users: evidence from positron emission tomography studies with [11C]WIN-35,428. J Neurosci 18:8417–8422

McKetin R, Kelly E, McLaren J (2006) The relationship between crystalline methamphetamine use and methamphetamine dependence. Drug Alcohol Depend 85:198–204

Michaluk P, Kolodziej L, Mioduszewska B, Wilczynski GM, Dzwonek J, Jaworski J, Gorecki DC, Ottersen OP, Kaczmarek L (2007) Beta-dystroglycan as a target for MMP-9, in response to enhanced neuronal activity. J Biol Chem 282:16036–16041

Mohammadi MT, Shid Moosavi SM, Dehghani GA (2011) Contribution of Nitric Oxide Synthase (NOS) activity in blood–brain barrier disruption and edema after acute ischemia/reperfusion in aortic coarctation-induced hypertensive rats. Iran Biomed J 15:22–30

Nair A, Bonneau RH (2006) Stress-induced elevation of glucocorti-
    coids increases microglia proliferation through NMDA receptor
    activation. J Neuroimmunol 171:72–85

Nitta T, Hata M, Gotoh S, Seo Y, Sasaki H, Hashimoto N, Furuse M,
    Tsukita S (2003) Size-selective loosening of the blood–brain
    barrier in claudin-5-deficient mice. J Cell Biol 161:653–660

Papadopoulos MC, Manley GT, Krishna S, Verkman AS (2004)
    Aquaporin-4 facilitates reabsorption of excess fluid in vasogenic
    brain edema. FASEB J 18:1291–1293

Park M, Hennig B, Toborek M (2012) Methamphetamine alters occlu-
    din expression via NADPH oxidase-induced oxidative insult and
    intact caveolae. J Cell Mol Med 16:362–375

Perry VH (2007) Stress primes microglia to the presence of systemic
    inflammation: implications for environmental influences on the
    brain. Brain Behav Immun 21:45–46

Quaegebeur A, Lange C, Carmeliet P (2011) The neurovascular link in
    health and disease: molecular mechanisms and therapeutic impli-
    cations. Neuron 71:406–424

Ramirez SH, Potula R, Fan S, Eidem T, Papugani A, Reichenbach N,
    Dykstra H, Weksler BB, Romero IA, Couraud PO, Persidsky Y
    (2009) Methamphetamine disrupts blood–brain barrier function
    by induction of oxidative stress in brain endothelial cells. J Cereb
    Blood Flow Metab 29:1933–1945

Ricaurte GA, Schuster CR, Seiden LS (1980) Long-term effects of
    repeated methylamphetamine administration on dopamine and
    serotonin neurons in the rat brain: a regional study. Brain Res
    193:153–163

Stein-Behrens B, Mattson MP, Chang I, Yeh M, Sapolsky R (1994)
    Stress exacerbates neuron loss and cytoskeletal pathology in the
    hippocampus. J Neurosci 14:5373–5380

Tata DA, Yamamoto BK (2007) Interactions between methamphetamine
    and environmental stress: role of oxidative stress, glutamate and
    mitochondrial dysfunction. Addiction 102(Suppl 1):49–60

Tata DA, Raudensky J, Yamamoto BK (2007) Augmentation of
    methamphetamine-induced toxicity in the rat striatum by unpre-
    dictable stress: contribution of enhanced hyperthermia. Eur J
    Neurosci 26:739–748

Thomas DM, Kuhn DM (2005) Cyclooxygenase-2 is an obligatory
    factor in methamphetamine-induced neurotoxicity. J Pharmacol
    Exp Ther 313:870–876

Thomas DM, Walker PD, Benjamins JA, Geddes TJ, Kuhn DM (2004)
    Methamphetamine neurotoxicity in dopamine nerve endings of
    the striatum is associated with microglial activation. J Pharmacol
    Exp Ther 311:1–7

Verkhratsky A, Olabarria M, Noristani HN, Yeh CY, Rodriguez JJ (2010)
    Astrocytes in Alzheimer's disease. Neurotherapeutics 7:399–412

Volkow ND, Chang L, Wang GJ, Fowler JS, Franceschi D, Sedler M,
    Gatley SJ, Miller E, Hitzemann R, Ding YS, Logan J (2001a)
    Loss of dopamine transporters in methamphetamine abusers
    recovers with protracted abstinence. J Neurosci 21:9414–9418

Volkow ND, Chang L, Wang GJ, Fowler JS, Leonido-Yee M, Franceschi
    D, Sedler MJ, Gatley SJ, Hitzemann R, Ding YS, Logan J, Wong C,
    Miller EN (2001b) Association of dopamine transporter reduction
    with psychomotor impairment in methamphetamine abusers. Am J
    Psychiatry 158:377–382

Wagner GC, Ricaurte GA, Seiden LS, Schuster CR, Miller RJ, Westley
    J (1980) Long-lasting depletions of striatal dopamine and loss of
    dopamine uptake sites following repeated administration of meth-
    amphetamine. Brain Res 181:151–160

Wolburg-Buchholz K, Mack AF, Steiner E, Pfeiffer F, Engelhardt B,
    Wolburg H (2009) Loss of astrocyte polarity marks blood–brain
    barrier impairment during experimental autoimmune encephalo-
    myelitis. Acta Neuropathol 118:219–233

Yamagata K, Andreasson KI, Kaufmann WE, Barnes CA, Worley PF
    (1993) Expression of a mitogen-inducible cyclooxygenase in
    brain neurons: regulation by synaptic activity and glucocorticoids.
    Neuron 11:371–386

Yamamoto BK, Zhu W (1998) The effects of methamphetamine on the
    production of free radicals and oxidative stress. J Pharmacol Exp
    Ther 287:107–114

Yamamoto M, Ramirez SH, Sato S, Kiyota T, Cerny RL, Kaibuchi K,
    Persidsky Y, Ikezu T (2008) Phosphorylation of claudin-5 and
    occludin by rho kinase in brain endothelial cells. Am J Pathol
    172:521–533

Yamamoto BK, Moszczynska A, Gudelsky GA (2010) Amphetamine
    toxicities: classical and emerging mechanisms. Ann N Y Acad Sci
    1187:101–121

Yang GY, Gong C, Qin Z, Liu XH, Lorris Betz A (1999) Tumor
    necrosis factor alpha expression produces increased blood–brain
    barrier permeability following temporary focal cerebral ischemia
    in mice. Brain Res Mol Brain Res 69:135–143

Yousif S, Marie-Claire C, Roux F, Scherrmann JM, Decleves X (2007)
    Expression of drug transporters at the blood–brain barrier using
    an optimized isolated rat brain microvessel strategy. Brain Res
    1134:1–11

Zhao C, Ling Z, Newman MB, Bhatia A, Carvey PM (2007) TNF-
    alpha knockout and minocycline treatment attenuates blood–brain
    barrier leakage in MPTP-treated mice. Neurobiol Dis 26:36–46